J. Plasma Physics (1999), *vol.* 62, *part* 5, *pp.* 513–529. Printed in the United Kingdom

Bifurcated equilibria in two-dimensional MHD with diamagnetic effects

C. TEBALDI[1] and M. OTTAVIANI[2]

[1]Department of Mathematics, University of Lecce, 73100 Lecce, Italy

[2]DRFC/SCCP, CEA Cadarache, 13108 St Paul lez Durance, France

(Received 1 December 1998 and in revised form 29 April 1999)

Abstract. In this work, we analyse the sequence of bifurcated equilibria in two-dimensional reduced magnetohydrodynamics. Diamagnetic effects are studied under the assumption of a constant equilibrium pressure gradient, not altered by the formation of a magnetic island. The formation of an island when the symmetric equilibrium becomes unstable is studied as a function of the tearing-mode stability parameter Δ' and of the diamagnetic frequency, by employing fixed-point numerical technique and an initial-value code. At larger values of Δ', a tangent bifurcation takes place, above which no small-island solutions exist. This bifurcation persists up to fairly large values of the diamagnetic frequency (of the order of one-tenth of the Alfvén frequency). The implications of this phenomenology for the intermittent MHD dynamics observed in tokamaks is discussed.

1. Introduction

A common feature of laboratory and space plasmas is the observation of intermittent enhancement of magnetohydrodynamic (MHD) activity. In the case of tokamak plasmas, one can include in this category of phenomena sawtooth relaxation, the so-called edge-localized modes (ELMs) occurring in high-confinement regimes, and, as extreme events, disruptions that lead to a sudden termination of the current discharge (Kadomtsev 1992). Sometimes these events are preceded by a well-identified *precursor*, namely the occurrence of an observable slowly growing magnetic island inside the plasma.

One of the problems encountered when trying to understand theoretically this phenomenology in tokamaks is that one usually finds that the excitations that break the symmetry of the initially axisymmetric state are of the 'soft' type. For values of some control parameter p slightly above the stability threshold p_c of the axisymmetric state, the system settles in a neighbouring state of slightly broken symmetry, for example an equilibrium with a small saturated magnetic island.

In certain situations, one can rule out the occurrence of a hard transition, directly from the symmetric equilibrium, on energetic grounds. This is when one can show that the amount of energy that can be released during the transition is proportional to some positive power of $p - p_c$. This energy thus tends to zero at the transition point. In this case, hard transitions are ruled out because they would require a finite release of energy at threshold.

The difficulty in understanding the frequently observed 'hard' excitations on the

basis of perturbation analysis around the *initially axisymmetric* state has become known as the 'trigger' problem (Wesson et al. 1991).

In general, abrupt changes of observable quantities are conveniently described in the conceptual framework of bifurcation theory (Guckenheimer and Holmes 1986). In particular, hard excitations can generically appear as a tangent (saddle-node) bifurcation or a subcritical (hard) Hopf-type bifurcation. Upon a slow variation of the control parameter, both types of bifurcations lead to abrupt ("catastrophic") changes in some observable quantity.

In a previous paper, Tebaldi et al. (1996) explored the possibility of overcoming the difficulty posed by the trigger problem by investigating the nature of a second bifurcation of the non-symmetric saturated state. This was done for a slab model of reduced resistive MHD (RRMHD), by varying the tearing-mode stability parameter Δ' as control parameter. (We recall that Δ' is defined as the jump in the logarithmic derivative of the eigenfunctions of linear ideal MHD across the singular layer, where resistivity becomes important.)

The main result was that, after a first bifurcation (occurring near $\Delta' = 0$) leading to a saturated tearing mode with a magnetic island of small amplitude, the system undergoes a tangent bifurcation at $L\Delta' \approx 1$, where L is a macroscopic scale length. Above this value of Δ', no equilibrium with a small island exists. The system jumps to a state where the island width is of the order of the system size.

To the extent that the island width is somewhat less than the system size, we expect the findings of Tebaldi et al. (1996) to be largely independent of geometry. Therefore they suggest a qualitative explanation of sudden reconnection events observed in laboratory plasmas. On the basis of our analysis, we proposed that these events would occur from a state of already-broken symmetry when the second bifurcation (a catastrophe) takes place. This state of slightly broken symmetry can be identified as the precursor state in which a small stable island can in principle be observed.

There are two main aims of this paper. The first is to carry out a more detailed analysis of the parametric dependence of the first bifurcated equilibrium than what was done in Tebaldi et al. (1996), by employing analytical perturbation theory and numerical methods. The second is to begin to study how the island is affected by the diamagnetic terms, by extending the previous model to include the drift velocity under the assumption of constant (frozen) pressure gradients.

For practical reasons, we shall still restrict our investigation to the two-dimensional (2D) MHD model, although it should be noted that, in principle, a complete analysis of the stability of islands would require the use of three-dimensional (3D) models, since further bifurcations can break the surviving symmetry. We find that the 2D phenomenology turns out to be sufficiently rich to be able to reproduce, at least qualitatively, some of the experimental observations.

Here we briefly review some of the previous literature.

An analytical calculation of the saturated island width had been carried out by Thyagaraja (1981) using an expansion in the parameter $\Delta' L$. The author found two coalescent solutions in the region where such an expansion breaks down ($\Delta' \approx 1/L$).

In another work, Wesson et al. (1985) considered tearing instabilities in cylindrical geometry. By heuristically modifying the linear eigenvalue problem to include the effect of the modification of the equilibrium field due to the island, an equation for the saturated island width of the form $\Delta'_{\mathrm{nonlinear}}(w) = 0$ was obtained. This equation has two solutions, which coalesce when a critical value of the current is reached.

Above this value, no solution exists. This was proposed as a possible mechanism for low-β disruptions.

However, one must stress that these results are perturbative, being essentially based on an expansion in the parameter Δ', which is only appropriate to treat the region around the first bifurcation. This expansion breaks down when approaching any subsequent bifurcation point. Thus any conclusion about the nature of a subsequent bifurcation can only be speculative when it is based on the methods of Thyagaraja (1981) and Wesson et al. (1985).

The analysis of Saramito and Maschke (1993) is valid beyond the first bifurcation. Those authors, however, considered only situations with constant slab aspect ratio and used S as a bifurcation parameter. In a later work, Parker et al. (1990) studied the bifurcation sequence in RRMHD with an initial-value code, using a variable slab aspect ratio at a constant Lundquist number ($S \approx 10^2$). No tangent bifurcation was detected in either work. It should be noted, however, that both investigations were carried out by employing rigid boundary conditions (zero radial flows at the walls). This choice strongly limits the island growth, since the radial flow far from the reconnecting region would normally tend to grow together with the island. Thus a more natural boundary condition would seem to be $\partial v_x/\partial x \to 0$.

This paper is organized as follows. Section 2 is devoted to the illustration of the MHD model and Sec. 3 to the numerical techniques. In Sec. 4, we review the stability analysis of the symmetric equilibrium. The bifurcation analysis for stationary islands is in Sec. 5 and the interpretation of these results is given in the Appendix. The case of a rotating island, still under investigation, is treated in Sec. 6. Conclusions and a discussion of possible developments are given in Sec. 7.

2. The MHD model

The MHD model used in this work is a generalization of single-helicity reduced resistive magnetohydrodynamics (RRMHD) (Kadomtsev and Pogutse 1974). The normalized model equations can be written as

$$\partial_t U + v^* \partial_y U + [\phi, U] = [J, \psi] + \mu \nabla^2 U, \tag{2.1}$$

$$\partial_t \psi + [\phi, \psi] = -\eta (J - J_0). \tag{2.2}$$

These equations are defined on a two-dimensional domain with coordinates x and y. With reference to the magnetic geometry of a tokamak, x can be thought of as a radial coordinate, labelling the equilibrium flux surfaces, and y as a poloidal coordinate. The third direction is considered ignorable. The model equations describe the evolution of the plasma vorticity $U = \nabla^2 \phi$, where ϕ is the electric potential (which plays the role of the stream function), and of the magnetic flux function ψ associated with the magnetic field in the plane (a constant magnetic field is assumed in the ignorable direction). The other fields in (2.1) and (2.2) are the current density $J = -\nabla^2 \psi$ and the equilibrium current density J_0, associated with the equilibrium flux function ψ_0. Moreover, for any two fields A and B, $[A, B] \equiv \partial_x A \partial_y B - \partial_y A \partial_x B$, so that $[\phi, \cdot] = \mathbf{v} \cdot \boldsymbol{\nabla}$ is the usual advection operator.

Lengths are normalized to a macroscopic length L, which is a measure either of the size of the system or of the scale length of the variation of the equilibrium magnetic field. Times are normalized to the Alfvén time $\tau_A = L/v_A$, where $v_A =$

https://doi.org/10.1017/S0022377899008120 Published online by Cambridge University Press

$B_p/\rho^{1/2}$ is the poloidal Alfvén speed associated with the equilibrium field B_p (ρ is the mass density).

The dissipation is measured by the viscosity μ and by the resistivity η, which, in these units, are respectively the inverses of the Reynolds number R, $\mu = 1/R$, and of the Lundquist number S (magnetic Reynolds number), $\eta = 1/S$.

In this simple model, the diamagnetic effect is measured by the equilibrium ion drift velocity v^*. The possible inclusion of the electron drift velocity v_e^* in Ohm's law would not alter qualitatively the behaviour of this model, as long as one neglects the evolution of the plasma pressure. In this case, v_e^* would appear in (2.2), as an additional term $v_e^* \partial_y \psi$. This term can be transformed away by going to a reference frame moving at the velocity v_e^*. Thus one does not lose generality by ignoring v_e^* in (2.2).

Of course, a more complete model would require the addition of a third equation for the plasma pressure (or temperature), which also would allow the analysis of the important effects of the nonlinearity in the diamagnetic terms. The treatment of this effect is, however, beyond the scope of this work. One should regard the analysis presented here as a first step towards understanding the role of the diamagnetic terms on the formation of magnetic islands.

The model given by (2.1) and (2.2) is completed by specifying the domain on which the dynamics takes place, the functional form of the equilibrium magnetic field and the boundary conditions. In the rest of this work, the domain is taken to be a square box (slab) $[-L_x, L_x] \times [-L_y, L_y]$, where the normalized lengths are of order one. It is convenient to take $L_x = \pi$ and $L_y = \pi/\epsilon$, where the slab aspect ratio ϵ has been introduced. The normalized equilibrium flux function is taken to be symmetric,

$$\psi_0 = \cos x. \tag{2.3}$$

Thus the magnetic field has a null along the line $x = 0$. One can anticipate that a magnetic island will develop around this line when the equilibrium is unstable.

The boundary conditions are taken to be periodic in both directions. Although periodicity is natural in the y direction, it seems somewhat odd to use it in the radial direction x. In reality, when the island width w is sufficiently smaller than the system size, $w \ll L_x$, the only effect of periodicity is to add a duplicate island around the line $x = \pm\pi$. When the islands are small, they do not interact. Far from the island, in the region around the lines $x = \pm\frac{1}{2}\pi$, there is no poloidal flow, but one must in general allow some radial flow, whose magnitude adjusts to the evolving island. Thus, when the island is sufficiently small, employing periodic boundary conditions is physically equivalent to imposing a freely evolving radial flow (with no poloidal flow) at the location $x = \pm\frac{1}{2}\pi$.

The dissipation coefficients are taken to be constant. In the case of the resistivity, this implies that the equilibrium electric field E_0 in the ignorable direction is not uniform, since $E_0 = \eta J_0$. We feel that this is a small price to pay for simplicity. Alternatively, one could take E_0 and η to be prescribed functions of x, or of the flux function ψ, as has been done by other authors. Note in particular that by chosing $E_0 = \text{const}$ and $\eta = \eta(\psi)$, one can construct solutions with exactly zero flow everywhere, as in Sykes and Wesson (1981). However, in this case, one has to specify the functional form $\eta(\psi)$ in a somewhat arbitrary manner. In reality, it seems to us that all the choices that one can make within a strictly two-field MHD model have some drawbacks. The point is of course that the resistivity is in principle

a function of the temperature. There is simply no way to determine it uniquely without the addition of at least a third equation for the electron temperature.

Thus the system of equations (2.1) and (2.2) is controlled by four dimensionless parameters. We choose ϵ, v^*, S and the magnetic Prandtl number $P = R/S$. In the rest of this paper, P is kept fixed, $P = 0.2$ (this value, chosen for numerical convenience, is somewhat larger than that given by Braginskii 1985).

3. Numerical techniques

Various numerical techniques were employed. When possible, fixed-point methods were used as an efficient way to track the sequence of equilibria, relying on bifurcation theory (which is predictive). In addition, a pseudospectral initial-value code was employed to benchmark the fixed-point calculations or when studying the transient dynamics. In some cases, transients were studied with an initial-value code employing a direct truncation of the model equations to the relevant degrees of freedom.

3.1. Fixed-point method

In order to solve the system of equations (2.1) and (2.2), a spectral decomposition is adopted for the unknowns, choosing the eigenfunctions of the Laplacian as the complete orthogonal set for the expansion. One has

$$(\phi, \psi) = \sum_{\mathbf{k}} (\phi_{\mathbf{k}}, \psi_{\mathbf{k}}) e^{i\mathbf{k}\cdot\mathbf{x}}, \qquad \mathbf{k} = (l, m\epsilon), \quad l \text{ and } m \text{ integers}. \tag{3.1}$$

We truncate the expansion to a finite set L of $2N$ wave vectors ('modes') such that if $\mathbf{k}$ belongs to L then $-\mathbf{k}$ also belongs to L. This gives $4N$ ordinary differential equations for $4N$ real unknowns. Moreover, in the special case $v^* = 0$, a $2N$-dimensional invariant subspace exists characterized by imaginary amplitudes for the magnetic and velocity fields, which allows one to reduce the system to $2N$ equations. Different sets L have been considered, starting from a 'ball' around the origin with $N = 100$ and adding modes in a slab centred at $m = 0$ up to $N = 200$.

The time-independent version of (2.1) and (2.2) can be cast in the form $\mathbf{F}(\mathbf{a}, \mathbf{p}) = 0$ where $\mathbf{a}$ are the unknowns and $\mathbf{p}$ the set of control parameters. A suitable tool to find the solutions is Newton's method, used in connection with the theorems of bifurcation theory (Tebaldi 1989). One should stress that the relevant features of the method are the capability of finding both stable and unstable equilibria and its efficiency in following the sequence of equilibria when parameters are varied. Unstable equilibria are also essential to obtain the bifurcation diagram and then to understand the dynamics in the nonlinear regimes.

3.2. Pseudospectral code

Since the model equations are supplemented with periodic boundary conditions, a suitable initial-value code is a spectral code, which advances in time the Fourier components of the relevant field. The code that we employed adopts the pseudospectral method to compute the nonlinear terms, which in Fourier space take the form of convolutions. After computing the derivatives in Fourier space, the fields are transformed to real space, where the nonlinearities are simple products at each grid point. The result is then transformed back to Fourier space. In this way, the number of operations needed to compute the nonlinearities scales like

$N \log N$ instead of the unfavourable scaling like N^2 that one would get with direct evaluation of the convolutions.

4. Stability of the symmetric equilibrium

It is known (Furth et al. 1963), that a symmetric magnetic configuration can be unstable to symmetry breaking perturbations under certain conditions. The stability boundary of the reference equilibrium can be obtained with linear theory by imposing the condition that the frequency be real. Upon writing $\phi = \tilde{\phi}(x)e^{-i\omega t+iky}$ and $\psi = \psi_0 + \tilde{\psi}(x)e^{-i\omega t+iky}$, and using (2.3), one obtains the linearized version of (2.1) and (2.2):

$$(\omega - \omega^*)\nabla^2\tilde{\phi} = k \sin x[\partial_x{}^2\tilde{\psi} + (1 - k^2)\tilde{\psi}] + i\mu\nabla^4\tilde{\phi}, \tag{4.1}$$

$$\omega\tilde{\psi} - k \sin x\, \tilde{\phi} = i\eta\nabla^2\tilde{\psi}, \tag{4.2}$$

where

$$\omega^* = v^*k, \qquad k = m\epsilon, \qquad \nabla^2 \equiv \partial_x{}^2 - k^2.$$

4.1. Stability when $v^* = 0$

The case $v^* = 0$ is made simpler by the fact that ω^2 is real. The reference equilibrium is destabilized when ω^2 goes through zero. The stability boundary is obtained by solving

$$0 = k \sin x[\partial_x{}^2\tilde{\psi} + (1 - k^2)\tilde{\psi}] + i\mu\nabla^4\tilde{\phi}, \tag{4.3}$$

$$-k \sin x\, \tilde{\phi} = i\eta\,(\partial_x{}^2\tilde{\psi} - k^2\tilde{\psi}). \tag{4.4}$$

As usual, these equations can be solved by asymptotic matching. Far from the lines $x = 0$ and $x = \pm\pi$, where the magnetic field vanishes, the solution of (4.3) and (4.4) is approximated by the solution of the outer equations

$$0 = \partial_x{}^2\tilde{\psi}_{\text{out}} + (1 - k^2)\tilde{\psi}_{\text{out}}, \tag{4.5}$$

$$-k \sin x\, \tilde{\phi}_{\text{out}} = i\eta\,(\partial_x{}^2\tilde{\psi}_{\text{out}} - k^2\tilde{\psi}_{\text{out}}). \tag{4.6}$$

The outer solutions depend on the sign of $\kappa^2 \equiv 1 - k^2$, being exponentials when $\kappa^2 < 0$ and sinusoids when $\kappa^2 \geqslant 0$. It turns out that only sinusoids can be matched to the solution of (4.3) and (4.4) in the region around $x = 0$ and $x = \pm\pi$ (the inner solution). These correspond to $k \leqslant 1$. When $k > 1$, no solution to (4.3) and (4.4) exists except the trivial one with zero amplitude. Thus $k > 1$ is a sufficient condition for the stability of the reference equilibrium. Since $k = m\epsilon$, with m a positive integer, this sufficient condition is $\epsilon > 1$. As ϵ decreases, the first instability occurs for mode number $m = 1$ at some $\epsilon \leqslant 1$. The corresponding outer solutions are conveniently chosen to be of the form

$$\tilde{\psi}_{\text{out}} = \bar{\psi} \cos \kappa(x + \tfrac{1}{2}\pi) \quad \text{for} \quad -\pi \ll x \ll 0, \tag{4.7}$$

$$\tilde{\psi}_{\text{out}} = \bar{\psi} \cos \kappa(x - \tfrac{1}{2}\pi) \quad \text{for} \quad 0 \ll x \ll \pi. \tag{4.8}$$

The parameter

$$\Delta' \equiv \lim_{x\to 0^+} \partial_x \log \tilde{\psi}_{\text{out}} - \lim_{x\to 0^-} \partial_x \log \tilde{\psi}_{\text{out}}$$

is usually introduced to discuss the stability condition. Thus

$$\Delta' = 2\kappa \tan(\tfrac{1}{2}\kappa\pi). \tag{4.9}$$

https://doi.org/10.1017/S0022377899008120 Published online by Cambridge University Press

This equation shows that, for the given equilibrium and for a given mode number m, there is a one-to-one correspondence between Δ' and the slab aspect ratio ϵ. Thus, throughout this paper, we shall use these two quantities interchangeably as a control parameter.

In the special case when $\mu = 0$, the outer equations must be extended to the points $x = 0$ and $x = \pm\pi$. Differentiability at these points requires $\kappa = 0$. Thus the stability boundary of the zero-viscosity case is

$$\Delta' = 0.$$

This is the usual result from tearing-mode theory (Furth et al. 1963) in the absence of viscosity. However, since $\tilde{\psi} = \bar{\psi}$, with $\bar{\psi}$ constant, the flow is singular in this case, $\tilde{\phi} = i\eta k\bar{\psi}/\sin x$. The role of the finite viscosity is to remove the singularity. At the same time, the stability boundary is shifted to some $\epsilon = \epsilon_c < 1$ or $\Delta' = \Delta'_c > 0$

The inner equations are obtained by approximating

$$\sin x \approx x, \qquad k \approx 1, \qquad \nabla^4\tilde{\phi} \approx \frac{d^4\tilde{\phi}}{dx^4}$$

and

$$\tilde{\psi} \approx \bar{\psi} \qquad \text{(constant-}\psi\text{ approximation)},$$

while $\partial_x^2\tilde{\psi}$ must be allowed to vary in the layer. The resulting equations depend on the arbitrary amplitude $\bar{\psi}$:

$$0 = x\partial_x^2\tilde{\psi}_{\text{in}} + i\mu\nabla^4\tilde{\phi}_{\text{in}}, \tag{4.10}$$

$$-x\tilde{\phi}_{\text{in}} = i\eta\,(\partial_x{}^2\tilde{\psi}_{\text{in}} - \bar{\psi}). \tag{4.11}$$

It is convenient to introduce the length $\delta = (\mu\eta)^{1/6}$ and to employ new normalizations $\xi \equiv \delta x$ and $\tilde{\phi}_{\text{in}}(x) \equiv (i\eta\bar{\psi}/\delta)g(\xi)$. One gets

$$\frac{d^4g(\xi)}{d\xi^4} + \xi^2 g(\xi) - \xi = 0, \tag{4.12}$$

$$\frac{d^2\tilde{\psi}_{\text{in}}}{dx^2} = \frac{\bar{\psi}}{\xi}\frac{d^4g(\xi)}{d\xi^4}. \tag{4.13}$$

By matching the logarithmic derivatives of $\tilde{\psi}_{\text{in}}$ and $\tilde{\psi}_{\text{out}}$, one determines the stability boundary:

$$\Delta'_c = \frac{1}{\bar{\psi}}\left(\frac{d\tilde{\psi}_{\text{in}}}{dx}\right)_{x\to\infty} = \delta\int_0^\infty d\xi\,\frac{1}{\xi}\frac{d^4g(\xi)}{d\xi^4}. \tag{4.14}$$

The integral on the right-hand side is finite since $g(\xi)$ is localized around $\xi \approx 1$. In order to compute the precise value of Δ'_c, one needs to solve (4.12). However, since the integral in (4.14) is a number, one can conclude that Δ'_c scales as δ:

$$\Delta'_c \sim \delta \sim P^{1/6}S^{-1/3}. \tag{4.15}$$

4.2. Stability when $v^* \neq 0$

When $v^* \neq 0$, the stability analysis is complicated by the fact that $\omega \neq 0$ at threshold and the phase difference between $\tilde{\phi}$ and $\tilde{\psi}$ is not just $\frac{1}{2}\pi$. The resulting equation has complex coefficients and depends on an additional parameter that cannot be absorbed in the normalizations. As a consequence, there seem to be no way to determine the functional dependence of Δ'_c on the dimensionless parameters

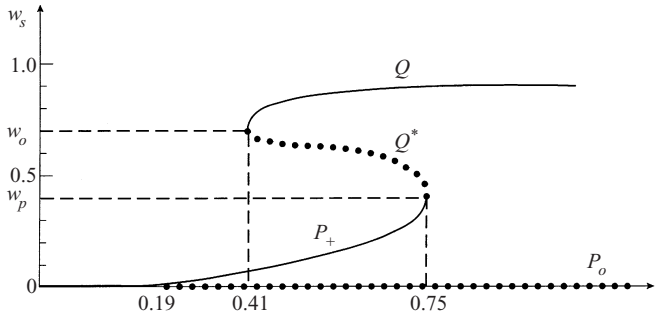

Figure 1. Normalized island width w_s for the equilibria P_o, P_+, Q and Q^* versus Δ' for $S = 1000$. Solid lines denote stability, dotted lines instability.

without completely solving the relevant linear problem. Some numerical results are reported in Sec. 6.

5. Results without diamagnetic effects

Previous results concerning the structure of the bifurcation diagram in the case $v^* = 0$ have been reported in Tebaldi et al. (1996). Here we summarize those results and report on a more detailed study of the scaling of the small-island solutions in the proximity of the first bifurcation at $\Delta' = \Delta'_c$.

5.1. Bifurcation diagram at $v^* = 0$

The sequence of equilibria with stationary magnetic islands when $v^* = 0$ was studied for $0 < \Delta' < 1.15$ and S up to 1000 using the fixed-point code. The results where found to be essentially unaffected by the truncation procedure. The main result is shown in Fig. 1, where the island width w for the different equilibria is plotted against Δ'. Stable and unstable equilibria are indicated by solid and dotted lines respectively.

As expected, the initial symmetric equilibrium with $w = 0$ (denoted by P_o) becomes unstable to tearing-like perturbation when $\Delta' = \Delta'_c = 0.19$. This value is consistent with the estimate given in (4.15). The bifurcation is a pitchfork, and a new stable equilibrium with a small magnetic island, denoted by P_+, appears. When $\Delta' = \Delta'_Q = 0.41$, a pair of equilibria – one stable (denoted by Q) and one unstable (Q^*) – appear via tangent bifurcation. At a higher value $\Delta' = \Delta'_P = 0.75$, another tangent bifurcation occurs, characterized by the coalescence of Q^* with the small-island solution P_+. Above this value, the only stable solution is Q.

For completeness, in Fig. 2, we show the contour plots of ψ and ϕ for the three equilibria P_+, Q^* and Q at a value of Δ' just under Δ'_P. One can see that in the case of P_+ the magnetic island retains approximately its linear shape. This is less so for the velocity field, which is, however, still organized in four main convective cells. By comparison, the island width of the Q equilibrium is comparable to the equilibrium scale length. The corresponding velocity field is more complicated, with four main elongated vortices aligned along the separatrices.

We also checked that, in the Δ' range under study, the bifurcation diagram is stable to a further increase of S. There are indications that the position of the tangent bifurcation points depend regularly on the resistivity (giving rise to small $O(1/S)$ corrections). On the other hand, the position of the symmetry-breaking

https://doi.org/10.1017/S0022377899008120 Published online by Cambridge University Press

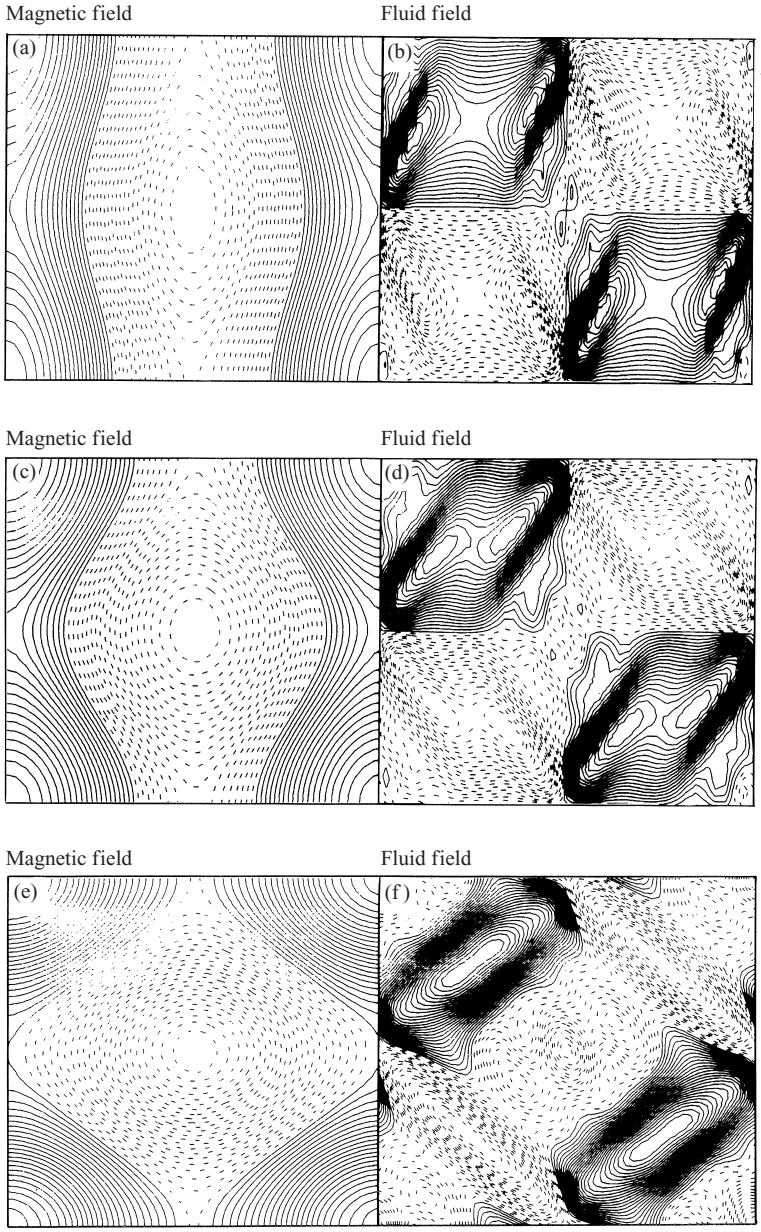

Figure 2. Contour plots of ψ and ϕ at Δ' slightly less than Δ'_P for P_+ (a, b), Q^* (c, d) and Q (e, f).

bifurcation depends non-regularly on the resistivity, with $\Delta'_c \sim S^{-1/3}$, as explained in the Appendix.

5.2. Scaling of the island width near Δ'_c

The behaviour of the island width in the small-island regime is shown in Figs 3–5. One can distinguish two regimes. The first, which occurs when the control parameter ϵ is just above the threshold of the symmetry-breaking bifurcation, is char-

https://doi.org/10.1017/S0022377899008120 Published online by Cambridge University Press

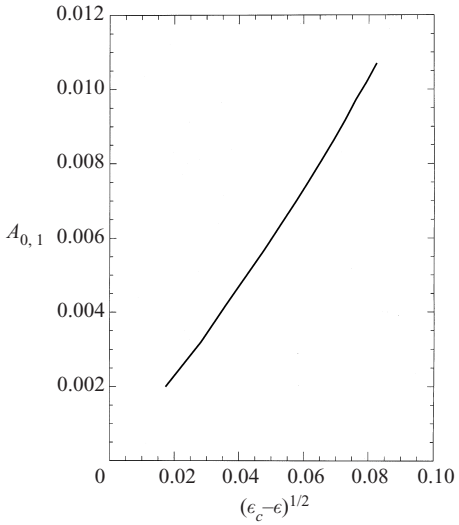

Figure 3. Amplitude of the $l = 0, m = 1$ component versus $(\epsilon_c - \epsilon)^{1/2}$ near threshold. $S = 1000$, $v^* = 0$. Square-root regime.

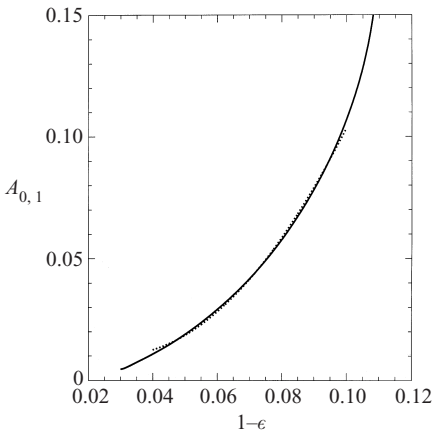

Figure 4. Log–log plot of the amplitude of the $l = 0, m = 1$ component versus ϵ near threshold. Quadratic regime and offset parabolic fit (dotted line).

acterized by a square-root dependence of the amplitude on the departure from threshold, as generally the case with this type of bifurcations. This is shown clearly in Fig. 3, where the amplitude $A_{0,1}$ of the $l = 0$, $m = 1$ mode, obtained by fixed-point calculations, is plotted against $(\epsilon_c - \epsilon)^{1/2}$.

For higher values of the amplitude, but still such that the island width is much smaller than the system size, the square-root behaviour turns into a quadratic dependence of $A_{0,1}$ on $1 - \epsilon$, so that the island width, which is proportional to $A_{0,1}^{1/2}$, scales linearly. In this regime, the relaxation towards the fixed points is sufficiently fast that one can track the whole portion of the $A_{0,1}$ versus $1 - \epsilon$ curve by using the initial-value code with a slowly varying ϵ. The result is shown in Fig. 4 (solid line). The dotted line represents the offset parabolic fit $A_{0,1} = 0.0102 + 18.34(1 - \epsilon)^2$ in the range $0.9 \leqslant \epsilon \leqslant 0.96$. The two scaling ranges are combined in Fig. 5.

https://doi.org/10.1017/S0022377899008120 Published online by Cambridge University Press

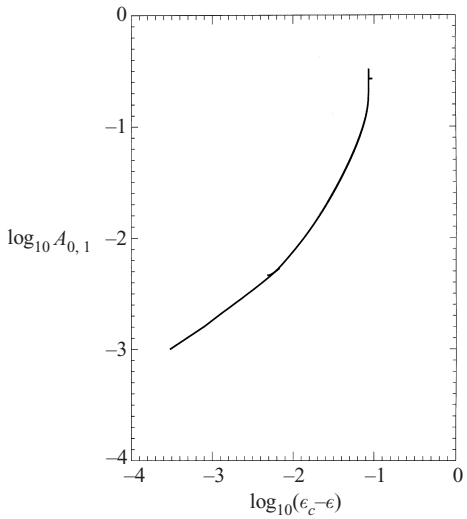

Figure 5. Amplitude of the $l = 0, m = 1$ component versus ϵ near threshold. Combined square-root and quadratic regimes.

6. Results with diamagnetic effects

As already mentioned in Sec. 3.1, the full $4N$-dimensional system of ordinary differential equations, $2N$ being the number of modes considered, has to be investigated in the general case $v^* \neq 0$.

Furthermore, as expected, the symmetric equilibrium becomes unstable because of a supercritical Hopf bifurcation, giving rise to a time-periodic solution. In general, the problem of investigating the existence and stability of periodic solutions is far more demanding than the one for equilibria, even if in principle the definition of a Poincaré map (Guckenheimer and Holmes 1986)] leads one to study the existence and stability of fixed points for the map, according to Floquet theory.

In our case, however, the problem can still be recast as a fixed-point one because the time-periodicity of the bifurcated state is only due to a rotation frequency for the island, like in a rigid-body rotation.

Equations (2.1) and (2.2) can be written in the form $\mathbf{F}(\mathbf{a}, \mathbf{p}, \omega) = \mathbf{0}$, where $\mathbf{a}$ are $4N - 1$ unknowns (there is an arbitrary phase) for the real Fourier amplitudes, ω is the unknown rotation frequency and p is the set of control parameters. Newton's method can still be used to find the solutions, but convergence turns out to be much slower than for the case $v^* = 0$, which seriously limits the possibility of investigation when dealing with large islands. In this case, the initial-value code was employed as a complementary tool.

Here we summarize how the bifurcation diagram is affected by the diamagnetic effects. The critical value ϵ_c at which the symmetric equilibrium undergoes the Hopf bifurcation is a decreasing function of v^*, i.e. the transition takes place at higher values of Δ'. This is consistent with the general notion that the diamagnetic effects are stabilizing when treated linearly, as is done in this work. (By comparison, nonlinear diamagnetic terms can be destabilizing in certain regimes, as in Samain (1984).) The rotation frequency of the island is an increasing function of v^*, but its magnitude at threshold is much smaller (by a factor of order 10^{-3}) than the diamagnetic frequency. Thus the transition condition is now represented by a critical

https://doi.org/10.1017/S0022377899008120 Published online by Cambridge University Press

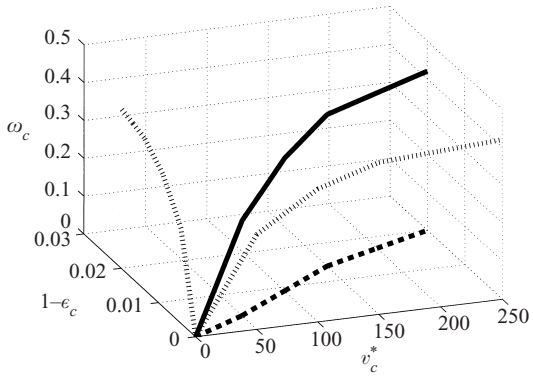

Figure 6. Plot of the angular frequency ω_c as a function of the control parameters v_c^* and $1-\epsilon_c$ (thick solid line), and the critical line in the $(v_c^*, 1-\epsilon_c)$ plane (thick dashed line). The thin dashed lines represent the projections of the ω_c curve on the (v_c^*, ω_c) and $(\omega_c, 1-\epsilon_c)$ planes.

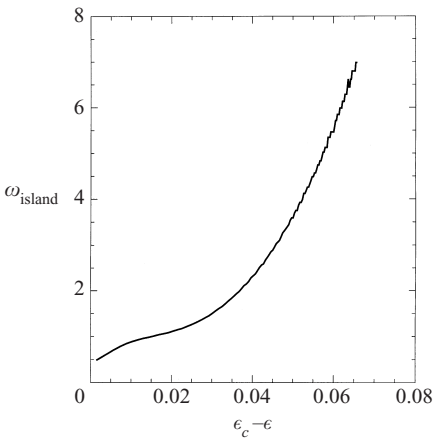

Figure 7. Angular frequency of the island as a function of ϵ ($v^* = 0.1$).

line in the (v^*, ϵ) plane. The results at threshold are summarized in Fig. 6, where the angular frequency ω_c of the island at its birth is plotted against the critical values of the two control parameters v_c^* and $1-\epsilon_c$ (thick solid line). Also shown is the critical line in the (v^*, ϵ) plane (thick dashed line) and the projections of the ω_c curve on the other two planes (thin dashed lines).

As one departs from threshold, the island rotates progressively faster, although its frequency stays significantly smaller than the diamagnetic frequency. The dependence of the angular frequency of the island in the case $v^* = 0.1$ is shown in Fig. 7. At constant, ϵ the size of the island is a decreasing function of v^*, again showing the stabilizing role of v^*.

The values of ϵ at which the two tangent bifurcations take place are also affected by v^*. As v^* grows, the two critical values become closer, until at some point the two tangent bifurcations coalesce and disappear (the S-shaped curve characteristic of the bifurcation diagram unfolds). This occurs at $v^* \approx 0.1$, i.e. for a diamagnetic velocity that is a factor 10 below the Alfvén speed. This phenomenon is clearly

https://doi.org/10.1017/S0022377899008120 Published online by Cambridge University Press

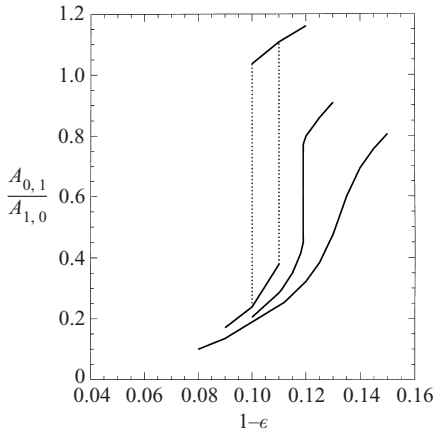

Figure 8. Bifurcation diagrams for the cases (from left to right) $v^* = 0.05$, $v^* = 0.1$ and $v^* = 0.15$.

shown in Fig. 8, where the bifurcation diagram is outlined for three cases $v^* = 0.05$, $v^* = 0.1$ and $v^* = 0.15$. At $v^* = 0.05$, there are still coexisting stable equilibria for certain values of ϵ, whereas a single-value equilibrium curve is found for $v^* = 0.15$.

7. Final discussion and conclusions

In this work, we have analysed the sequence of the first bifurcations in two-dimensional resistive MHD. The role of the ion diamagnetic frequency on the island dynamics has also been considered, in a simplified way.

Perturbation calculations have confirmed and clarified the numerical results obtained in Tebaldi et al. (1996) for the stability analysis of the symmetric equilibria and for the parameter scalings of the bifurcated one.

The analysis of the sequence of bifurcations in the presence of the diamagnetic effect, although still in a preliminary stage, has confirmed qualitatively the bifurcation diagram obtained in Tebaldi et al. (1996), up to a critical value of the diamagnetic velocity v_c^* (of the order of one-tenth of the Alfvén speed). Thus the disappearance of moderately large islands because of a tangent bifurcation as a possible mechanism for 'hard' excitations is confirmed also in the case of island rotation.

As far as the actual time scale of the hard transition is concerned, this depends simultaneously on the intrinsic time scale associated with the dynamics around the tangent bifurcation and on the time scale at which the control parameter changes. The generic equation in normal form near the tangent bifurcation is

$$\frac{d\xi}{dt} = \xi^2 + \delta p, \tag{7.1}$$

where ξ is a coordinate on the centre manifold and δp is the deviation of the control parameter from the bifurcation point. This equation is normalized, but it is reasonable to conjecture that, for the present MHD problem, the time would be normalized to the Alfvén time. If we assume that δp evolves around zero at some slower time scale, for example $d\delta p/dt = \eta \ll 1$, then a rescaling of (7.1) shows that ξ departs substantially (mathematically, it would go to infinity) from $\xi = 0$ in a time

https://doi.org/10.1017/S0022377899008120 Published online by Cambridge University Press

of order $t_\xi \sim \eta^{1/3} \ll \eta$. In the present MHD problem, δp is essentially Δ', so, in most experimental situations, η would be the inverse of the current diffusion time and the hard transition would take place in a time proportional to $S^{1/3}$ (in Alfvén time units), much faster than the current profile evolution time.

The different choice of boundary conditions is, in our view, the reason why our results differ from previous investigations by Saramito and Maschke (1993) and Parker et al. (1990) of a similar problem, where rigid boundary conditions at the wall, which force the radial flow to zero, were adopted.

We stress that our approach, being based on a fixed-point method, differs from most of the previous nonlinear analyses, which were traditionally carried out as initial-value problems, typically by deriving an approximate equation for the island dynamics, and by following the growth of an island from the neighbourhood of an unstable symmetric equilibrium. However, where the comparison is possible, we find that, in general, our results are consistent (at least qualitatively) with the information provided by such analyses.

The initial-value approach in the small-Δ' ($\ll 1/L$) limit leads to classic algebraic Rutherford growth (Rutherford 1973), followed by island saturation on the resistive time scale (White et al. 1977; Dagazian and Paris 1986). The scaling of the small-island size above the first bifurcation given in White et al. (1977), as a function of Δ', agrees with our findings.

For very large $\Delta' \gg (1/L)S^{1/3}$, the island is expected to reach the macroscopic size on the Sweet–Parker time scale (Sweet 1958; Parker 1957), while in the intermediate regime $1/L \ll \Delta' \ll (1/L)S^{1/3}$, Waelbroeck (1993) has shown that a transition between Rutherford and Sweet–Parker regimes occurs. Therefore, on the basis of the work of Waelbroeck (1993), no saturation is expected for $\Delta' L$ exceeding some critical value of order unity, which again is consistent with our finding of a tangent bifurcation at $\Delta' L \approx 1$, above which no small-island solution exists.

The advantage of the fixed-point method is that it is better suited for analysing the nature of the bifurcations, since it provides also information on the unstable equilibria. Furthermore, it avoids the difficulty, encountered by the initial-value approach, that, near the bifurcations, the natural time scales become extremely long.

One may ask how generic our findings could be if one were, for example, to consider a different geometry with realistic (tokamak-type) boundary conditions. As a general guideline, one expects that, whenever the island size is sufficiently smaller than the system size, the phenomenology observed in our model should be universal. In this respect, we regard the choice of periodic boundary conditions, originally dictated by numerical convenience, to be acceptably close to the realistic, free-boundary, conditions that one should, in principle, employ in cylindrical or toroidal geometry. We stress that the occurrence of tangent bifurcations in dynamical systems is generic, and therefore stable to small modifications of the system. On the other hand, one should be aware that additional phenomena can in principle appear in fully 3D geometry, where new degrees of freedom are allowed. If additional, intrinsically 3D, bifurcations were to appear before the tangent bifurcation then this would change the phenomenology described in this work. A 3D stability analysis of the 2D saturated islands is required to address this question.

Since our original motivation was to study the intermittent MHD phenomena observed in tokamaks, a natural question is what happens in reality when those hard events take place. Strictly speaking, on the basis of our analysis, one would be

tempted to conclude that a true disruption takes place, as in Wesson et al. (1985), since we find that, after the tangent bifurcation, the final state has an island of macroscopic size.

However, one should also consider that RRMHD gives only a partial description of the plasma. In particular, the fast transport processes occurring during the crash are not described by our model (at the very least, a third equation for the temperature should be added to describe this situation). These processes could introduce a feedback in the system that limits the growth of the magnetic island. If this were the case then intermittent relaxation events like ELMs would occur. In this respect, it is worth recalling that a tangent bifurcation is the basic ingredient of a common intermittency scenario in fluids (Pomeau and Manneville 1980).

Acknowledgements

The authors acknowledge productive discussions with F. Porcelli and useful comments by M. Zabiego. C.T. would like to thank the kind hospitality of the JET Joint Undertaking, where part of the work was carried out.

Appendix. Interpretation of the results without diamagnetic effects

In this appendix, we study analytically the dependence of the small-island solution on the departure from the stability boundary of the symmetric equilibrium.

The usual approach to obtain small-amplitude solutions above the symmetry-breaking point is based on a simultaneous expansion of the deviations from the symmetric equilibrium, $\tilde{\psi}$ and $\tilde{\phi}$, and of the control parameter, Δ', in terms of a new smallness parameter λ:

$$\tilde{\psi} = \lambda a_1 + \lambda^2 a_2 + \dots , \tag{A 1}$$

$$\tilde{\phi} = \lambda b_1 + \lambda^2 b_2 + \dots , \tag{A 2}$$

$$\Delta' = \Delta'_c + \lambda c_1 + \lambda^2 c_2 + \dots \quad . \tag{A 3}$$

These expansions are then inserted into the original equations. A sequence of conditions between the coefficients is obtained by matching equal powers in λ. Eventually, the series (A 3) is inverted to the desired order in $\Delta' - \Delta'_c$, and the expression for λ is inserted back into the expansions for $\tilde{\psi}$ and $\tilde{\phi}$. Here we only summarize the main findings with this procedure.

To the lowest order, one obtains the linear theory at threshold, which determines Δ'_c and the functional form of a_1 and b_1 (an overall amplitude is left arbitrary). To the next order, the symmetry of the reference equilibrium dictates that $c_1 = 0$. Thus, to the leading order, $\lambda \sim (\Delta' - \Delta'_c)^{1/2}$ and $\tilde{\psi} \sim (\Delta' - \Delta'_c)^{1/2}$ from (A 1). Thus the island width w_s scales as

$$w_s \approx 2\tilde{\psi}^{1/2} \sim (\Delta' - \Delta'_c)^{1/4}. \tag{A 4}$$

The higher-order coefficients a_2 and b_2 are found to be large (divergent) in the limit of small dissipation ($\mu \to 0$, $\eta \to 0$). This implies that the expansion breaks down at sufficiently large $\Delta' - \Delta'_c$. One can trace the breakdown to the near singularity of the linear solutions a_1 and b_1 around $x = 0$ when the dissipation is small. The role of the dissipation is to regularize such a singularity. Thus one expects the expansion to break down when the island width exceeds the dissipative layer width:

$w_s > \delta$, or

$$\Delta' - \Delta'_c \approx (\eta\mu)^{2/3} \tag{A 5}$$

Above this value, the singularity in the outer solutions is resolved by the nonlinearity in the layer. The island width then replaces δ as the layer width.

For larger-island solutions, pertinent to the situation of Fig. 4, the problem is conveniently treated by quasilinear (QL) theory. In QL theory, the interactions between the modes with $m \neq 0$ are neglected. The only nonlinear effect is the quasilinear modification of the symmetric equilibrium. The first consequence of the fact that $m \neq 0$ modes do not interact is that only modes that are linearly unstable acquire non-zero amplitude. Thus, in a neighbourhood of the stability threshold of the $m = 1$ mode, one can neglect the $m > 1$ modes, and the perturbed fields can be approximated as

$$\tilde{\psi} = \tilde{\psi}_0 + \tilde{\psi}_1 \cos \epsilon y, \tag{A 6}$$

$$\tilde{\phi} = \eta\tilde{\phi}_1 \sin \epsilon y. \tag{A 7}$$

In (A 7) the latter equation, the stream function has been explicitly rescaled by the factor η.

Upon substitution into the original model equations (2.1) and (2.2), one obtains a set of three ordinary differential equations for the three unknowns $\tilde{\psi}_0$, $\tilde{\psi}_1$ and $\tilde{\phi}_1$:

$$0 = (\psi'_0 + \tilde{\psi}'_0)(\tilde{\psi}''_1 - k^2\tilde{\psi}_1) - \tilde{\psi}_1(\psi'''_0 + \tilde{\psi}'''_0), \tag{A 8}$$

$$-\tilde{\phi}_1(\psi'_0 + \tilde{\psi}'_0) = \tilde{\psi}''_1 - k^2\tilde{\psi}_1, \tag{A 9}$$

$$-\tilde{\phi}'_1\tilde{\psi}_1 - \tilde{\phi}_1\tilde{\psi}'_1 = 2\tilde{\psi}''_0, \tag{A 10}$$

where the contribution of the vorticity nonlinearity has been suppressed in (A 8) since it vanishes as $\eta \to 0$. Equation (A 10) can be integrated to give

$$\tilde{\psi}'_0 = -\tfrac{1}{2}\tilde{\phi}_1\tilde{\psi}_1, \tag{A 11}$$

where the integration constant is zero because of the boundary conditions. Using (A 11) one can determine that, when the island width is small, $\tilde{\psi}'_0/\psi'_0 \ll 1$ uniformly and $\tilde{\psi}'_0$ can be neglected when it appears in the combination $\psi'_0 + \tilde{\psi}'_0$ (this can be verified a posteriori). Thus (A 8)–(A 10) are simplified to

$$0 = \psi'_0(\tilde{\psi}''_1 - k^2\tilde{\psi}_1) - \tilde{\psi}_1\psi'''_0 - \tilde{\psi}_1\tilde{\psi}'''_0, \tag{A 12}$$

$$-\tilde{\phi}_1\psi'_0 = \tilde{\psi}''_1 - k^2\tilde{\psi}_1, \tag{A 13}$$

$$\tilde{\psi}'_0 = -\tfrac{1}{2}\tilde{\phi}_1\tilde{\psi}_1. \tag{A 14}$$

In the small-island expansion combined with the constant-ψ approximation $\tilde{\psi}''_1 \sim \tilde{\psi}_1$ and $\tilde{\psi}'_1 \sim \kappa\tilde{\psi}_1 \ll \tilde{\psi}_1$. Thus, taking the second derivative of (A 14), one has, to the leading order, $\tilde{\psi}'''_0 = -\frac{1}{2}\tilde{\phi}''_1\tilde{\psi}_1$. Inserting this into (A 12) and eliminating $\tilde{\psi}''_1$ using (A 13) finally yields a single inhomogeneous linear equation for $\tilde{\phi}_1$:

$$\tfrac{1}{2}A^2\partial_x^2\tilde{\phi}_1 - x^2\tilde{\phi}_1 - Ax = 0, \tag{A 15}$$

where again the constant-ψ approximation has been used by taking $\tilde{\psi}_1 = A = \text{const}$, and the derivatives of the equilibrium field have been approximated by their expressions around the singular layer, $\psi'_0 = -\sin x \approx x$, etc.

The unknown amplitude A, which plays the role of an eigenvalue, is determined

by matching with the outer solution. This condition can be written as

$$\Delta' = \int_0^\infty dx\,(A + x\tilde{\phi}_1). \tag{A 16}$$

Finally, one can eliminate A from (A 15) by rescaling $\tilde{\phi}_= A^{1/2} g(x/A^{1/2})$. This makes explicit that the natural scale length in the layer is $A^{1/2}$, which is essentially the island width. The matching condition (A 16) becomes $\Delta' \approx A^{1/2}$, which is equivalent to the quadratic scaling of Fig. 4.

References

Braginskii, S. I. 1985 In: *Reviews of Plasma Physics*, Vol. 1 (ed. M. A. Leontovich), p. 285. Consultants Bureau, New York.

Dagazian, R. Y. and Paris, R. B. 1986 *Phys. Fluids* **29**, 762.

Furth, H. P., Killeen J. and Rosenbluth, M. N. 1963 *Phys. Fluids* **6**, 459.

Guckenheimer, J. and Holmes, P. 1986 *Nonlinear Oscillations, Dynamical Systems and Bifurcations of Vector Fields*. Springer-Verlag, New York.

Kadomtsev, B. B. 1992 *Tokamak Plasma: A Complex System*. Institute of Physics Publishing, Bristol.

Kadomtsev, B. B. and Pogutse, O. P. 1974 *Soviet Phys. JETP* **38** 283.

Parker, E. N. 1957 *J. Geophys. Res.* **62**, 509.

Parker, R. D., Dewar, R. L. and Johnson, J. L. 1990 *Phys. Fluids* **B2**, 508.

Pomeau Y. and Manneville, P. 1980 *Commun. Math. Phys.* **74**, 189.

Rutherford, P. H. 1973 *Phys. Fluids* **16**, 1903.

Samain, A. 1984 *Plasma Phys. Contr. Fusion* **26**, 731.

Saramito, B. and Maschke, E. K. 1993 In: *Magnetic Turbulence and Transport* (ed. P. Hennequin and M. A. Dubois), p. 33. Editions de Physique, Orsay.

Sweet, P. A. 1958 In: *Electromagnetic Phenomena in Cosmic Physics* (ed. B. Lehnert), p. 123. Cambridge University Press.

Sykes, A. and Wesson, J. A. 1980. In: *Proceeding of the 8th International Conference on Plasma Physics and Controlled Nuclear Fusion Research*, Vol. 1, p. 237. IAEA, Vienna.

Tebaldi, C. 1989 In: *Nonlinear Dynamics*, p. 412. World Scientific, Singapore.

Tebaldi, C., Ottaviani, M. and Porcelli, F. 1996 *Plasma Phys. Contr. Fusion* **38**, 619.

Thyagaraja, A. 1981 *Phys. Fluids* **24**, 1716.

Waelbroeck, F. L. 1993 *Phys. Rev. Lett.* **70**, 3259.

Wesson, J. A., Sykes, A. and Turner, M. F. 1985 In: *Proceeding of the 10th International Conference on Plasma Physics and Controlled Nuclear Fusion Research*, Vol. 2, p. 23. IAEA, Vienna.

Wesson, J. A., Edwards, A. W. and Granetz, R. S. 1991 *Nucl. Fusion* **31**, 111.

White, R. B., Monticello, D. A., Rosenbluth, M. N. and Waddell, B. V. 1977 *Phys. Fluids* **20**, 800.